



Mitigation of cisplatin-induced cardiotoxicity by Isorhamnetin: Mechanistic insights into oxidative stress, inflammation, and apoptosis modulation

Rawan Abudalo^a, Omar Gammoh^b, Sara Altaber^c, Yousra Bseiso^c, Esam Qnais^c, Mohammed Wedyan^c, Muna Oqal^d, Abdelrahim Alqudah^{a,*}

^a Department of Clinical Pharmacy and Pharmacy Practice, Faculty of Pharmaceutical Sciences, The Hashemite University, Zarqa 13133, Jordan

^b Department of Clinical Pharmacy and Pharmacy Practice, Faculty of Pharmacy, Yarmouk University, Irbid 21163, Jordan

^c Department of Biology and Biotechnology, Faculty of Science, The Hashemite University, Zarqa 13133, Jordan

^d Department of Pharmaceutics and Pharmaceutical Technology, Faculty of Pharmaceutical Sciences, The Hashemite University, Zarqa 13133, Jordan

ARTICLE INFO

Handling Editor: Prof. L.H. Lash

Keywords:

Isorhamnetin

Cisplatin

Cardiotoxicity

Nrf2

Oxidative stress

Inflammation

Apoptosis

ABSTRACT

The flavonoid compound Isorhamnetin (IRMN) is known for its considerable pharmacological properties, which include antioxidant and anti-inflammatory effects, as well as significant protective actions on heart health. However, the potential of IRMN to guard against heart damage caused by cisplatin (CP), a common chemotherapeutic agent, and the specific mechanisms involved, remain unexplored areas. This research was designed to investigate how IRMN counters CP-induced heart toxicity. In our study, mice were orally given IRMN at 50 or 150 mg/kg/day for a week, followed by CP injections (5 mg/kg/day) on the third and sixth days. The animals were euthanized under sodium pentobarbital anesthesia (50 mg/kg, intraperitoneally) on the eighth day to collect blood and heart tissues for further examination. Our findings reveal that IRMN administration significantly reduced the heart damage and the elevation of heart injury markers such as cardiac troponin I, creatine kinase, and lactate dehydrogenase induced by CP. IRMN also effectively lowered oxidative stress markers, including reactive oxygen species and malondialdehyde, while boosting ATP production and antioxidants like superoxide dismutase, catalase, and glutathione. The compound's capability to diminish the levels of pro-inflammatory cytokines like tumor necrosis factor- α and interleukin-6, alongside modulating apoptosis-regulating proteins (enhancing Bcl-2 while suppressing Bax and Caspase-3 expression), further underscores its cardioprotective effect. Notably, IRMN modulated the p62-Keap1-Nrf2 signaling pathway, suggesting a mechanism through which it exerts its protective effects against CP-induced cardiac injury. These insights underscore the potential of IRMN as an effective adjunct in cancer therapy, offering a strategy to mitigate the cardiotoxic side effects of cisplatin.

1. Introduction

Cisplatin (CP) is renowned for its ability to combat tumor cells through senescence induction or the activation of intrinsic apoptotic pathways, leading to non-repairable DNA damage [1]. Despite being the cornerstone of first-line cancer therapies, its clinical application is significantly limited by dose-dependent cardiotoxic effects, including arrhythmias, chest pain, and heart failure [2]. Such side effects can substantially elevate the risk of cardiovascular disorders in cancer patients undergoing CP treatment. Although the precise mechanisms underlying CP-induced heart toxicity are not fully elucidated, oxidative stress, inflammation, and apoptosis are recognized as key contributors to

its deleterious cardiac impacts.

The central factor driving CP-related cardiac injury is oxidative stress, marked by a disequilibrium between the production of reactive oxygen species (ROS) and antioxidant defense capabilities [3]. This oxidative imbalance is known to influence various cellular pathways, including those leading to inflammation and cell death [4]. Elevated ROS can activate nuclear transcription factors, leading to increased pro-inflammatory cytokine levels, thereby intensifying inflammatory responses [5]. Additionally, the surge in ROS production can compromise mitochondrial integrity, precipitating mitochondrial dysfunction, which in turn triggers the caspase-dependent apoptotic pathway [6]. The nuclear factor erythroid 2-related factor 2 (Nrf2) is crucial for

* Corresponding author.

E-mail address: Abdelrahim@hu.edu.jo (A. Alqudah).

<https://doi.org/10.1016/j.toxrep.2024.05.003>

Received 1 April 2024; Received in revised form 28 April 2024; Accepted 8 May 2024

Available online 12 May 2024

2214-7500/© 2024 The Author(s). Published by Elsevier B.V. This is an open access article under the CC BY-NC-ND license (<http://creativecommons.org/licenses/by-nc-nd/4.0/>).

cellular defense against oxidative damage [7]. The stabilization and activation of Nrf2, facilitated by p62-mediated sequestration of Keap1—a regulator of Nrf2 degradation—play a vital role in cellular resilience to oxidative stress and apoptotic signaling [8].

Isorhamnetin (IRMN), a flavonoid with extensive pharmacological properties, including antioxidative, anti-inflammatory, and cardioprotective effects, has been the focus of recent research [9]. Studies have demonstrated IRMN's efficacy in reducing myocardial injury following ischemia/reperfusion by curbing lactate dehydrogenase (LDH)-related apoptosis via the NF- κ B pathway [10]. Moreover, IRMN has been found to inhibit angiotensin II-induced cardiac fibroblast proliferation and collagen production, offering a protective mechanism against myocardial fibrosis [9]. Additionally, its effectiveness in diminishing myocardial collagen buildup and fibrosis in diabetic models through the inhibition of the TGF- β /Smad pathway highlights IRMN's therapeutic potential in cardiac fibrosis management [11].

This research evaluates the cardioprotective properties of IRMN against CP-induced toxicity in mice, focusing on alterations in cardiac histopathology and myocardial biomarker levels. It also delves into the associated mechanisms by analyzing markers of oxidative stress, inflammation, apoptosis, and the involvement of the p62–Keap1–Nrf2 signaling axis.

2. Materials and methods

2.1. Animal preparation

In this study, we utilized fifty male mice, each weighing between 20 and 25 g. These animals were housed under controlled environmental conditions, with temperatures maintained at 22–25 °C and relative humidity kept within 40%–60%. Access to a standard diet and clean water was provided *ad libitum* for a duration of one week before the initiation of experimental procedures. The ethical approval for conducting this study was obtained from the ethics committee at the Hashemite University, Zarqa, Jordan, with the approval number 14/4/2021/2022 dated 14 April 2022. Our research adhered strictly to the ARRIVE guidelines to promote the responsible and ethical conduct of animal-based research [12].

2.2. Experimental design and drug administration

The study involved the division of the fifty mice into five distinct groups, with each group consisting of ten mice. The groups were designated as follows: Control, CP (Cisplatin), L-IRMN (Low-dose Isorhamnetin + CP), H-IRMN (High-dose Isorhamnetin + CP), and IRMN alone. Mice in the CP group were subjected to intraperitoneal injections of CP at a dosage of 5 mg/kg. The dose of 5 mg/kg for CP used in your study is within the range of dosages typically used in research to induce toxicity without being lethal. Such dosages are commonly chosen to study sub-lethal nephrotoxic effects while avoiding more severe, potentially lethal outcomes associated with higher doses. Research indicates that a range of doses from low sub-therapeutic (5 mg/kg) to sub-lethal nephrotoxic (10–12 mg/kg) are used, depending on the severity of nephrotoxicity and other side effects being studied [13]. The L-IRMN and H-IRMN groups were treated with oral doses of IRMN at concentrations of 50 mg/kg and 150 mg/kg, respectively, in combination with CP at 5 mg/kg. The IRMN-only group received an oral dose of 150 mg/kg of IRMN. The specific doses of IRMN (50 mg/kg and 150 mg/kg) used correspond to a range tested in preliminary studies for efficacy and safety in similar biochemical pathways as those influenced by CP. In pharmacological studies, the dose selection often varies widely based on the compound's potency, the route of administration, and the specific therapeutic targets [9,14]. The treatment regimen was maintained for a period of 7 days, with CP injections administered on the 3rd and 6th days and daily oral doses of IRMN. All substances used, including CP and IRMN, were sourced from SigmaAldrich, UK.

Following the last IRMN treatment, the mice were anesthetized using sodium pentobarbital at a dose of 50 mg/kg (i.p.), and then blood and heart tissues were collected for further analysis.

2.3. Histopathological examination

Following the collection of blood specimens, hearts were immediately excised and fixed in 4% paraformaldehyde solution for preservation. The heart tissues were then dehydrated and embedded in paraffin using standard techniques, forming solid paraffin blocks. Sections of 4 μ m thickness were sliced from these blocks and stained with hematoxylin and eosin (H&E) for detailed histological evaluation [15]. The analysis of histopathological changes was conducted using a Leica DM4000B optical microscope (Solms, Germany). Quantification of myocardial damage was performed with the aid of Image Pro Plus version 6.0 software.

2.4. Biochemical analysis

2.4.1. Serum biochemical analysis

Whole blood was centrifuged at a speed of 3500 rpm for a duration of 10 minutes at ambient temperature, to separate the serum [16]. The clear supernatant obtained was then stored at –20 °C until further biochemical evaluations were performed. The concentrations of serum creatine kinase (CK) and lactate dehydrogenase (LDH) were determined by adhering to the protocols specified by the kit manufacturer (Abcam, United Kingdom). CK assay employs the enzymatic conversion of creatine to phosphocreatine and ADP by CK. The resultant ADP reacts with a specific enzyme mix, forming a colorimetric product measurable at 450 nm. Sample and standards are added to wells, followed by the reaction mix, and analyzed kinetically using a microplate reader at 37 °C. This method allows for precise activity measurements and is adaptable for high-throughput screening [17]. LDH catalyzes the conversion of lactate to pyruvate, generating a colorimetric product detectable at 450 nm. This kit is suitable for assessing cell injury and cytotoxicity, featuring a straightforward protocol where samples are incubated with the LDH reaction mixture and read spectrophotometrically [18].

2.4.2. Cardiac tissue biochemical analysis

Heart tissue samples were processed by homogenization in a solution consisting of 0.9% saline to achieve a 10% (w/v) homogenate. This mixture was centrifuged at 3000 rpm for 10 minutes to separate the supernatant, which was used for the biochemical assays [19]. The activity levels of antioxidants including superoxide dismutase (SOD), catalase (CAT), and glutathione (GSH), as well as the lipid peroxidation marker malondialdehyde (MDA), were quantified in the heart tissue using assay kits provided by Abcam, United Kingdom. SOD assay employs a colorimetric technique to determine SOD activity, which is crucial for understanding oxidative stress in biological samples. The assay quantifies SOD's ability to catalyze the dismutation of superoxide radicals, indirectly measured through a formazan dye formed by superoxide reaction with a tetrazolium salt. This sensitive method provides a clear readout of SOD activity, essential for antioxidant research [20]. Catalase activity was measured using a colorimetric detection method that assesses the decomposition of hydrogen peroxide, a reaction catalyzed by catalase. The decrease in hydrogen peroxide concentration is directly proportional to the catalase activity in the sample. The assay setup involves the addition of sample to a reaction mixture containing hydrogen peroxide, followed by measurement of the absorbance decrease, reflecting catalase activity [21]. GSH quantifies total glutathione levels using a colorimetric approach. The assay relies on the enzymatic recycling method, where glutathione reductase reduces oxidized glutathione in the presence of NADPH, which is then measured colorimetrically. This method provides a comprehensive view of cellular antioxidant capacity and is pivotal for studies involving oxidative stress [22]. MDA Assay Kit offers a method to measure MDA, a marker of lipid

peroxidation, using a colorimetric assay. MDA reacts with thiobarbituric acid to form a pink adduct measured spectrophotometrically. This assay is crucial for assessing oxidative stress and damage in biological samples, providing a reliable measurement of lipid peroxidation levels [23].

2.4.3. Fluorescent imaging for reactive oxygen species detection

Heart tissues, freshly procured, were prepared for sectioning by embedding in optimal cutting temperature compound and then sectioned using a cryostat. To evaluate the levels of reactive oxygen species (ROS) in cardiac cells, sections were incubated with dihydroethidium (obtained from Sigma Chemical Co., USA) for 30 minutes at 37°C in an environment shielded from light. Following this, sections were further stained with DAPI (from Sigma Chemical Co., USA) for 10 minutes at ambient temperature, also avoiding light exposure [24]. DAPI staining marked the nuclei in blue, whereas ROS activity was visualized in red through fluorescein labeling. A Leica DM4000B fluorescence microscope (Solms, Germany) was utilized for examining and documenting the stained sections. For quantitative analysis of ROS levels captured in the images, Image-Pro Plus software version 6.0 (Media Cybernetics, Inc.) was used.

2.4.4. Determination of ATP content

ATP levels were determined using commercially available kit (Abcam, UK), following the instructions provided by the manufacturer. The samples were combined with the reaction mix and incubated at 37°C for 30 minutes. Subsequently, a precipitant was introduced and spun at 4000 rpm for 5 minutes. Afterward, the supernatant was treated with a coloring agent for 2 minutes, followed by the addition of a terminator at ambient temperature for another 5 minutes. The final absorbance was recorded at 636 nm using a microplate reader.

2.4.5. Enzyme-linked immunosorbent assay (ELISA)

The concentrations of cardiac troponin I (cTnI) in the serum and the levels of tumor necrosis factor- α (TNF- α) and interleukin-6 (IL-6) in cardiac tissues were quantitatively assessed. These measurements were carried out using specific ELISA kits [25] obtained from Sigma Chemical Company, USA, for cTnI, and Thermo Fisher Scientific, USA, for TNF- α , with IL-6 kits also sourced from Sigma. The procedure was strictly adhered to as per the guidelines provided with each kit to ensure accurate and reliable results. The kits utilize a sandwich ELISA format, where capture antibodies specific to the target proteins are pre-coated onto microplates. Samples and standards are incubated on these plates to bind the target proteins, followed by the addition of a detection antibody linked to an enzyme that produces a colorimetric readout proportional to the protein concentration.

2.4.6. Protein expression analysis via western blot

To analyze protein expression, heart tissues were processed by homogenization in RIPA buffer supplied by SigmaAldrich, UK, followed by centrifugation at 12,000 rpm for 10 minutes at a temperature of 4 °C, facilitating the protein extraction process. Proteins in equal concentrations were then electrophoresed using 10% SDS-PAGE and subsequently blotted onto PVDF membranes provided by Bio-Rad, UK. To prevent non-specific binding, membranes were immersed in a blocking solution containing 5% skimmed milk for a period of 2 hours at ambient temperature [26]. They were then probed overnight at 4 °C with primary antibodies at a 1:1000 dilution directed against B-cell lymphoma-2 (Bcl-2), Bcl-2-associated X protein (Bax), Caspase-3, p62, Keap1, and Nrf2, all of which were acquired from Abcam, UK. β -actin was utilized as a loading control, diluted at 1:10,000. The following day, after three TBST washes, the membranes were exposed to respective secondary antibodies at a dilution of 1:10,000 for an hour in a dark environment at room temperature. Post three additional washes, the protein bands were visualized using the ChemiDoc Western blotting detection apparatus from Bio-Rad, UK.

2.5. Statistical analysis

The analysis of the gathered data was conducted using Graphpad Prism software, with results being articulated as the mean \pm standard deviation (SD). A one-way analysis of variance (ANOVA) with subsequent Tukey's post hoc test was applied to determine the statistical disparities among the experimental groups. A threshold of $p < 0.05$ was set to denote statistical significance.

3. Results

3.1. Influence of IRMN on cardiac histopathological changes

As illustrated in Fig. 2, analysis of heart tissue histopathology revealed that both the control and exclusive IRMN treatment groups maintained typical histological structures. In contrast, the CP-treated group showed significant histopathological changes, including the presence of inflammatory cells, signs of cell apoptosis, and myocardial edema. Remarkably, these pathological changes were progressively diminished in both the low-dose IRMN (L-IRMN) and high-dose IRMN (H-IRMN) groups, demonstrating a clear dose-responsive improvement when compared to the CP-only group, with statistical significance noted ($p < 0.01$). This indicates the potent capability of IRMN to counteract the adverse effects of CP on heart tissue, specifically reducing inflammation, edema in myocardial cells, and preventing cell apoptosis.

3.2. Impact of IRMN on serum myocardial biomarkers

Presented in Fig. 3, the serum analysis highlights that the concentrations of myocardial biomarkers, specifically cardiac troponin I (cTnI) in Fig. 3A, creatine kinase (CK) in Fig. 3B, and lactate dehydrogenase (LDH) in Fig. 3C, were notably higher in the CP-treated group than in the control group, showing statistical significance ($p < 0.01$). Conversely, in groups treated with low-dose and high-dose IRMN (L-IRMN and H-IRMN, respectively), there was a significant decrease in the levels of these markers when compared to the CP-only group, indicating a dose-responsive improvement ($p < 0.05$ and 0.01 , respectively). The IRMN-alone group's biomarker levels were comparable to those of the control group, with no significant statistical difference ($p > 0.05$), suggesting that IRMN treatment alone does not adversely affect these myocardial markers.

3.3. IRMN's modulation of ROS

Fluorescence microscopy analysis, as indicated in Fig. 4, showed a pronounced elevation in ROS generation within the CP-treated group, significantly differing from the control group's results ($p < 0.01$). Conversely, treatment with both low and high doses of IRMN (L-IRMN and H-IRMN groups) was associated with a substantial decrease in ROS levels in comparison to the CP-only group, with this reduction being statistically significant ($p < 0.01$). Furthermore, the ROS levels in the group treated with IRMN alone were found to be comparable to those in the control group, with no significant difference noted ($p > 0.05$).



Fig. 1. : Chemical structure of isorhamnetin.[45].

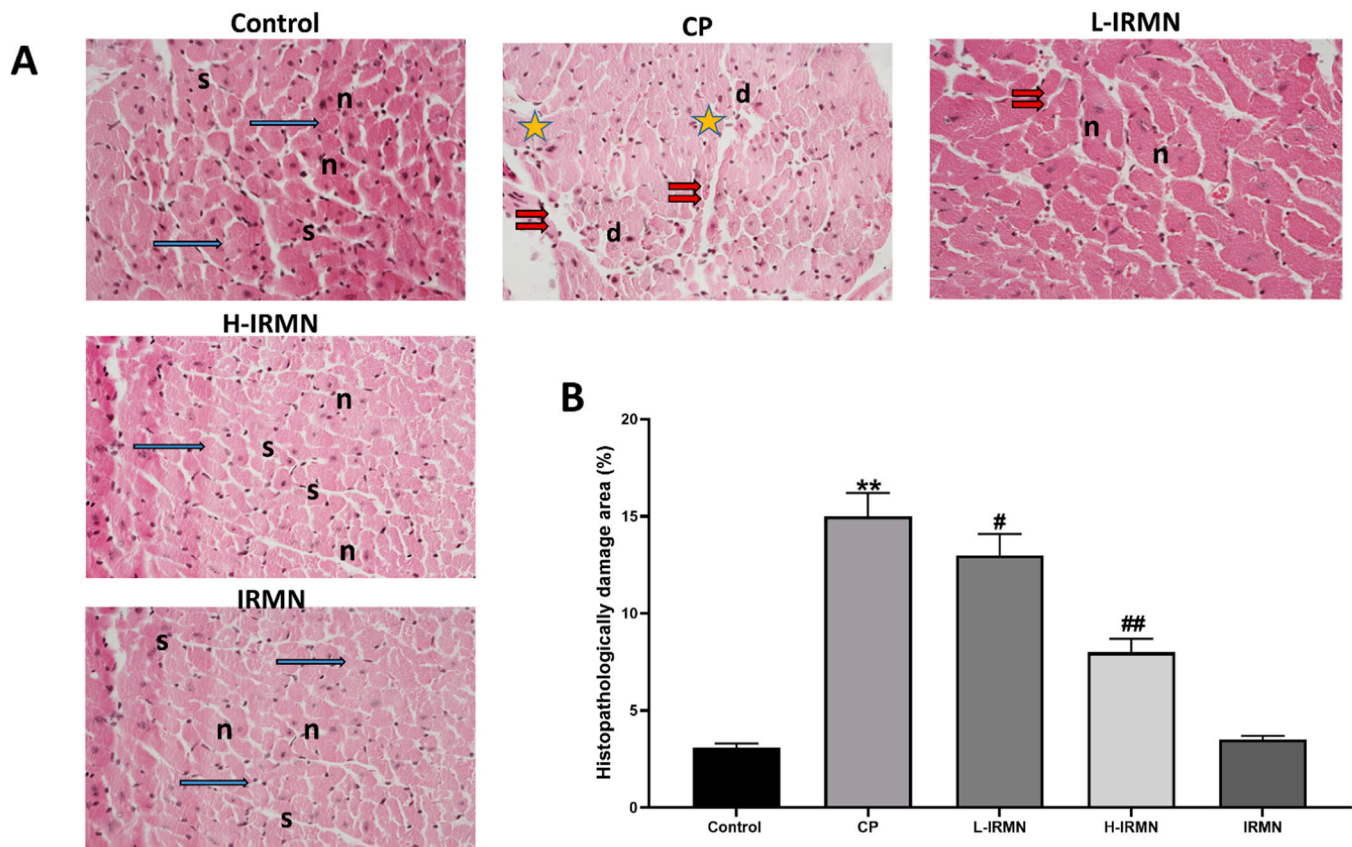


Fig. 2. : The impact of IRMN on cardiac histopathological alterations in mice induced with CP. Panel (A) displays H&E stain images for the control, CP, L-IRMN, H-IRMN, and IRMN groups, with a scale bar of 50 μm and a magnification of $\times 400$. Control group displays normal histology, where the arrow points to striated eosinophilic sarcoplasm and 'n' indicates central vesicular nuclei, with interstitial spaces marked by 's.' CP group exhibits numerous pathological features, including double arrows highlighting increased cell spacing and congested capillaries, while 'stars' denote periventricular infiltration by inflammatory cells, and 'd' marks deeply stained pyknotic nuclei. L-IRMN and CP treated group shows myofibrils that are more compact with narrower interstitial spaces. H-IRMN and CP treated group, there is a reduction in nuclear degeneration; myofibrils are normal with central nuclei indicated by (n) and consistently narrow interstitial spaces (s). In Panel (B), the myocardial injury area was quantified for each group. The arrows (1–3) indicate inflammatory cells, apoptotic cells, and myocardial edema cells, respectively. The data are expressed as the mean \pm SD for each group (n = 10). ** p < 0.01 compared to the control group; # p < 0.05 and ## p < 0.01 compared to the CP group.

3.4. Impact of IRMN on ATP content in mice

Fig. 5 showed a pronounced reduction in ATP content within the CP-treated group, significantly differing from the control group's results (p < 0.01). Conversely, treatment with both low and high doses of IRMN (L-IRMN and H-IRMN groups) was associated with a significant increase in ATP production in comparison to the CP-only group (p < 0.05, < 0.01, respectively). Furthermore, the ATP production in the group treated with IRMN alone were found to be comparable to those in the control group, with no significant difference noted (p > 0.05).

Top of Form

3.5. Influence of IRMN on oxidative stress and antioxidant defense markers

The examination of cardiac tissue for oxidative and antioxidant markers revealed distinct changes across the groups, as shown in Fig. 6. Specifically, in the CP-treated group, there was a notable decrease in the antioxidant enzymes SOD, CAT, and GSH (p < 0.01), alongside an increase in MDA, a marker of lipid peroxidation (p < 0.01), when compared to the control group. On the other hand, treatment with IRMN at both low (L-IRMN) and high (H-IRMN) doses resulted in elevated levels of SOD, CAT, and GSH, indicating enhanced antioxidant defense compared to the CP-only group (p < 0.05 or p < 0.01). Furthermore, the MDA levels were significantly lowered in the groups treated with IRMN,

reflecting reduced oxidative stress (p < 0.01). The group receiving IRMN alone demonstrated antioxidant and oxidative marker levels similar to those of the control group, with no significant variations observed (p > 0.05).

3.6. IRMN's impact on inflammatory cytokine levels

ELISA assessments demonstrated a pronounced elevation in the levels of the inflammatory cytokines TNF- α and IL-6 within the CP-treated group, significantly exceeding those of the control group (p < 0.01; depicted in Fig. 7). In contrast, interventions with IRMN at both low (L-IRMN) and high (H-IRMN) dosages resulted in a substantial reduction in TNF- α and IL-6 concentrations compared to the CP-only treated group (p < 0.01). Moreover, the levels of these cytokines in the group treated solely with IRMN were comparable to those in the control group, indicating no significant deviation (p > 0.05).

3.7. IRMN's influence on apoptotic protein expression

Western blotting aimed at analyzing apoptotic markers showed in the CP group a pronounced increase in the expression levels of pro-apoptotic proteins Bax and Caspase-3, alongside a decrease in anti-apoptotic Bcl-2 expression, all significantly diverging from control levels (p < 0.01, as seen in Fig. 8). In stark contrast, both low-dose (L-IRMN) and high-dose (H-IRMN) IRMN treatments resulted in a

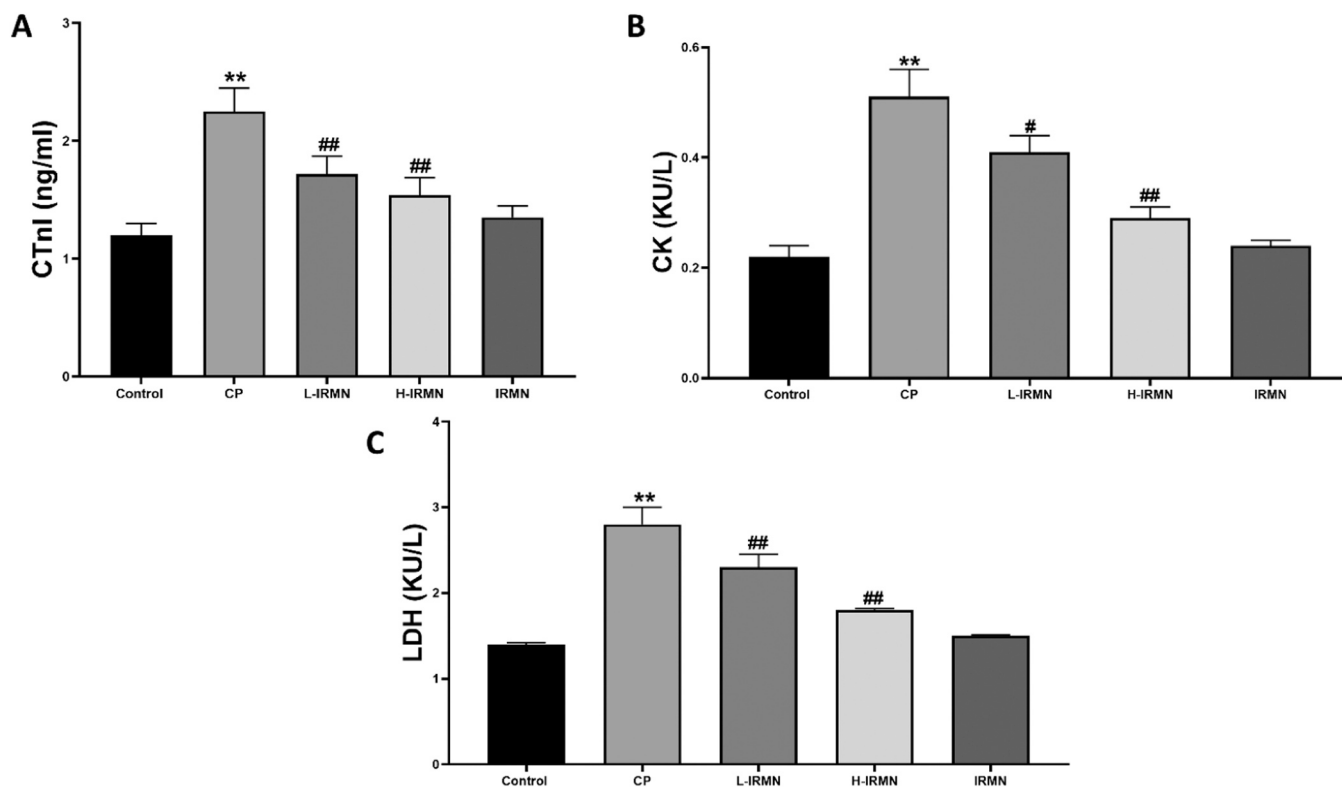


Fig. 3. : The influence of IRMN on the serum levels of myocardial markers, including cTnI (A), CK (B), and LDH (C), in mice induced with CP. The data are depicted as the mean ± SD for each group (n = 10). ** p < 0.01 compared to the CONT group; # p < 0.05 and ## p < 0.01 compared to the CP group.

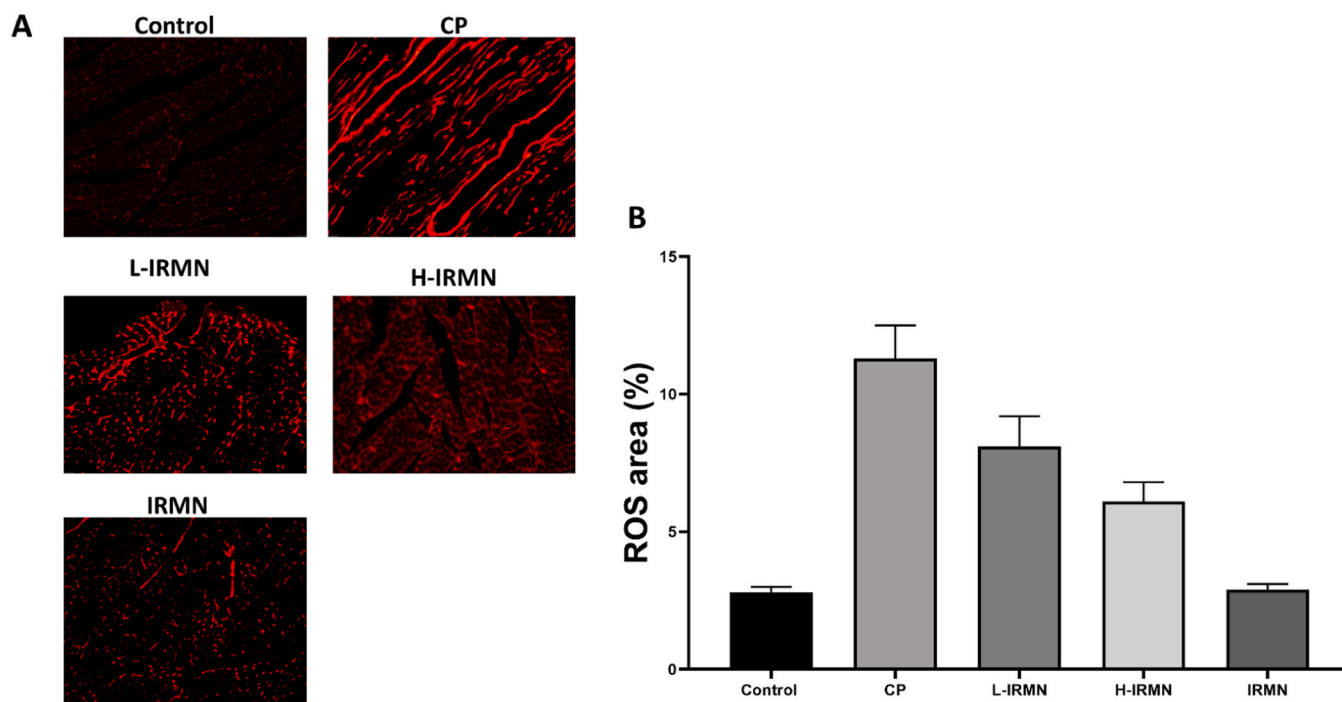


Fig. 4. : The impact of IRMN on the level of reactive oxygen species (ROS) in mice induced with CP. In Panel (A), representative images of ROS expression are shown for the CONT, CP, L-IRMN, H-IRMN, and IRMN groups, with a scale bar of 50 μm. Panel (B) presents the ROS fluorescent area, and the data are expressed as the mean ± SD for each group (n = 10). ** p < 0.01 compared to the control group; ## p < 0.01 compared to the CP group.

noticeable modulation of these markers towards a protective profile: Bax and Caspase-3 levels were markedly reduced, whereas Bcl-2 levels were elevated when compared with the CP-treated group (with statistical

significance at p < 0.05 or p < 0.01). Between the IRMN-only treated group and the control, the differences in the expression of these apoptotic markers were not statistically significant (p > 0.05),

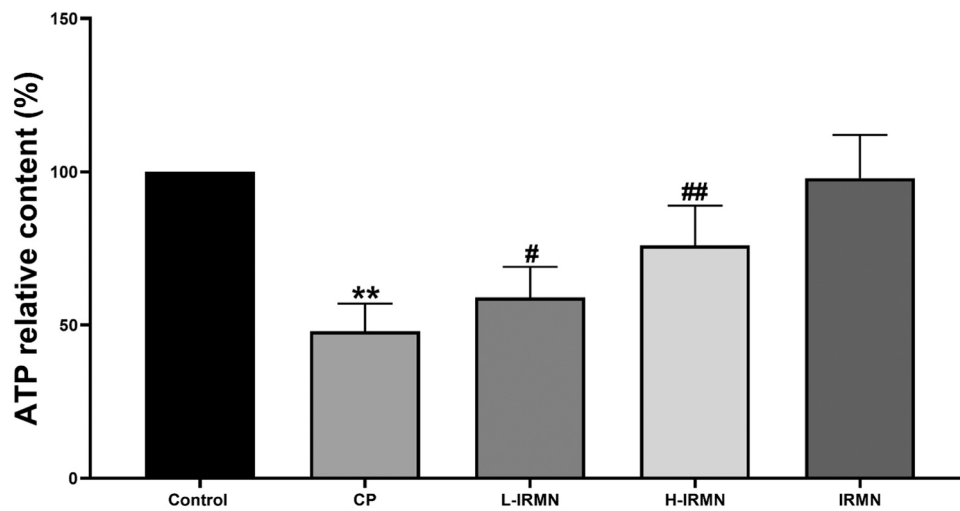


Fig. 5. : The influence of IRMN on ATP content. The data are presented as the mean \pm SD for each group (n = 6). ** p < 0.01 compared to the CONT group; # p < 0.05 and ## p < 0.01 compared to the CP group.

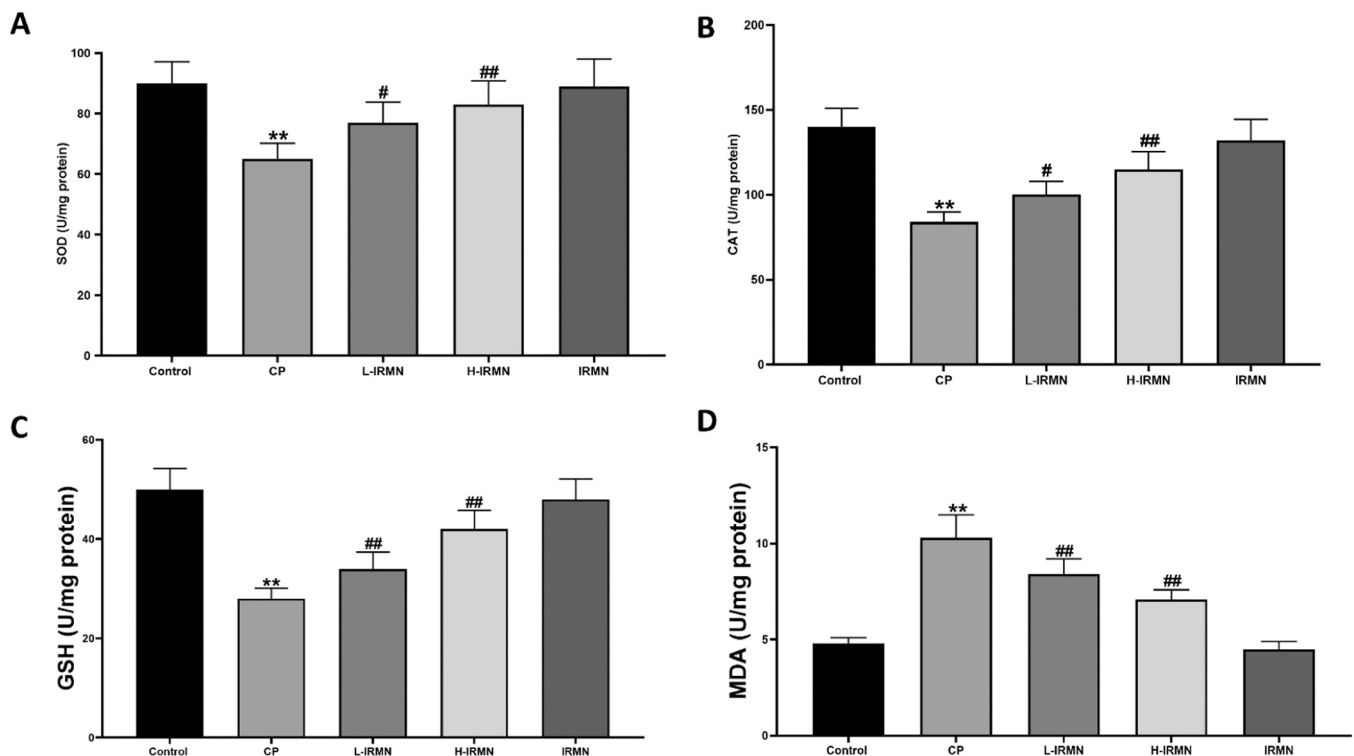


Fig. 6. : The influence of IRMN on the tissue levels of oxidative stress markers, including SOD (A), CAT (B), GSH (C), and MDA (D), in mice induced with CP. The data are presented as the mean \pm SD for each group (n = 6). ** p < 0.01 compared to the CONT group; # p < 0.05 and ## p < 0.01 compared to the CP group.

suggesting that IRMN, in the absence of CP-induced stress, does not affect the apoptotic balance.

3.8. Impact of IRMN on p62, Nrf2, and Keap1 protein expression

Western blot results highlighted in Fig. 9 show alterations in the signaling pathway proteins following treatment. Specifically, in the CP-treated group, there was a significant reduction in the expression of p62 and Nrf2 proteins (p < 0.01), accompanied by an elevation in Keap1 expression when compared to the control group. On the other hand, both the low-dose (L-IRMN) and high-dose (H-IRMN) IRMN treatments

resulted in an increase in p62 and Nrf2 levels (p < 0.05 or p < 0.01), alongside a decrease in Keap1 expression, compared to the CP group. Between the group treated with IRMN alone and the control, there were no noticeable differences in the expression levels of these proteins (p > 0.05), indicating that IRMN treatment, in the absence of CP challenge, does not significantly alter the expression of these key signaling molecules.

4. Discussion

The significant cardiotoxic side effects of Cisplatin (CP), along with

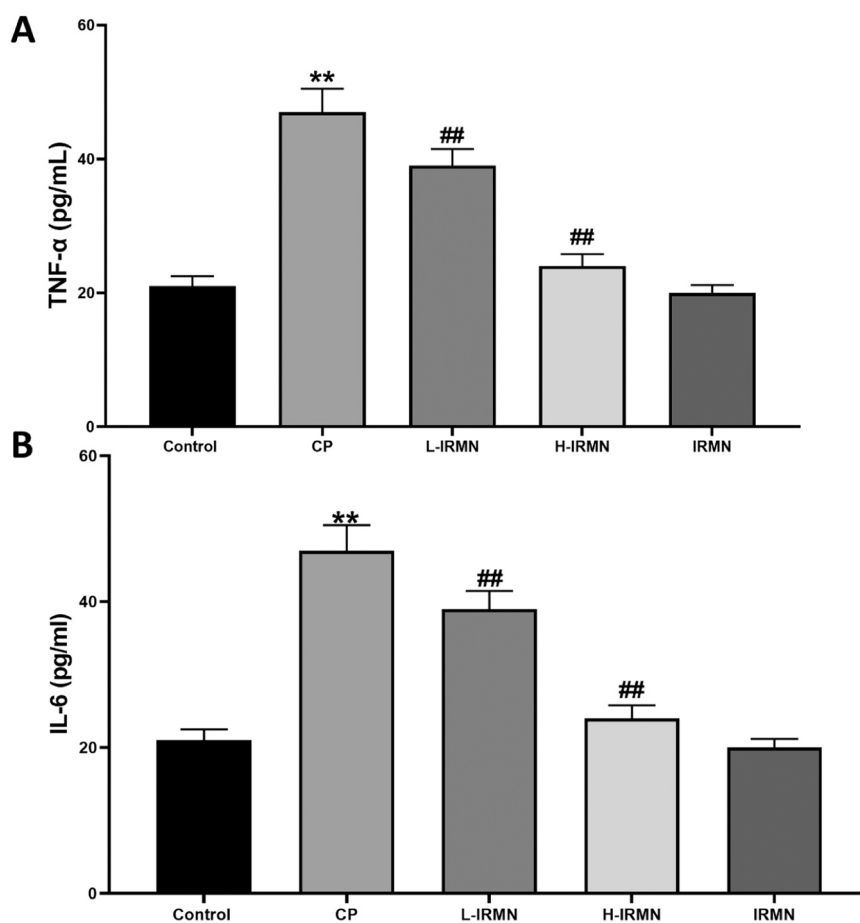


Fig. 7. : The impact of IRMN on the levels of the inflammatory cytokines TNF- α (A) and IL-6 (B) in mice induced with CP. The data are presented as the mean \pm SD for each group (n = 10). ** p < 0.01 compared to the CONT group; ## p < 0.01 compared to the CP group.

its other adverse reactions, pose a substantial challenge in cancer therapy, compelling many patients to discontinue its use prematurely [27, 28]. This disruption often prevents patients from realizing the full potential of their cancer treatment, underscoring an urgent need for safer, cardioprotective therapeutic strategies. Isorhamnetin, a naturally occurring flavonoid recognized for its broad pharmacological benefits, presents a promising avenue for mitigating CP's detrimental effects on the heart.

The cardioprotective capacity of isorhamnetin is not only hypothesized but also supported by substantial *in vitro* and *in vivo* evidence. Previous studies have established its protective effects on vital organs such as the liver [29], lungs [30], and kidneys [31] from various damages. Yet, the specific impact of isorhamnetin on cardiac tissue, particularly against CP-induced toxicity, and the underlying mechanisms remain less explored. Our study bridges this gap, demonstrating through histopathological evaluations how isorhamnetin ameliorates CP-induced pathological changes in the heart, including inflammation, cellular edema, and apoptosis. Notably, these protective effects were dose-dependent, with higher doses of isorhamnetin offering more significant protection.

Biochemical markers like Cardiac Troponin I (CTnI), Creatine Kinase (CK), and Lactate Dehydrogenase (LDH) are pivotal in diagnosing cardiac injury [32]. The elevation of these markers in response to CP treatment, as observed in our study, indicates cardiac damage. Conversely, isorhamnetin treatment significantly attenuated the levels of these markers, suggesting a protective mechanism against CP-induced cardiac toxicity. This finding aligns with the hypothesis that isorhamnetin mitigates membrane damage and functional impairment, primarily through its antioxidative actions.

Oxidative stress, characterized by an imbalance between the production of reactive oxygen species (ROS) and the body's antioxidant capacity, plays a central role in CP-induced cardiac damage [33]. Enzymatic antioxidants such as SOD, CAT, and GSH are crucial in mitigating oxidative stress. An increase in ROS can diminish SOD and CAT activity, causing oxidative stress. GSH, an essential antioxidant, becomes depleted, further increasing ROS activity and triggering a series of lipid peroxidation that compromises membrane integrity. MDA, a byproduct of lipid peroxidation, indicates the extent of damage to biological tissues [34]. Elevated MDA levels can severely damage cell membranes, increasing oxidative stress. Our study illustrates that CP treatment disrupts the balance of these antioxidants, exacerbating oxidative stress and cellular damage. Isorhamnetin's intervention, which elevates SOD, CAT, and GSH levels while reducing MDA, underscores its potential to restore this balance, thus protecting cardiac cells from oxidative damage.

The interplay between oxidative stress and inflammation is a key driver of CP-induced cardiotoxicity. ROS overproduction can trigger inflammatory responses, further aggravating cardiac damage [35]. TNF- α , a crucial inflammatory cytokine, can initiate an inflammatory cascade, contributing to myocardial apoptosis and ventricular remodeling, while IL-6 can lead to cardiac depression [36,37]. Previous research has shown that CP increases TNF- α and IL-6 release in heart tissue, contributing directly to damage [38]. Our findings that isorhamnetin significantly lowers inflammatory cytokines TNF- α and IL-6 further validate its anti-inflammatory properties. This dual action of combating oxidative stress and inflammation underscores isorhamnetin's comprehensive cardioprotective mechanism.

Moreover, evidence suggests CP causes severe heart toxicity by

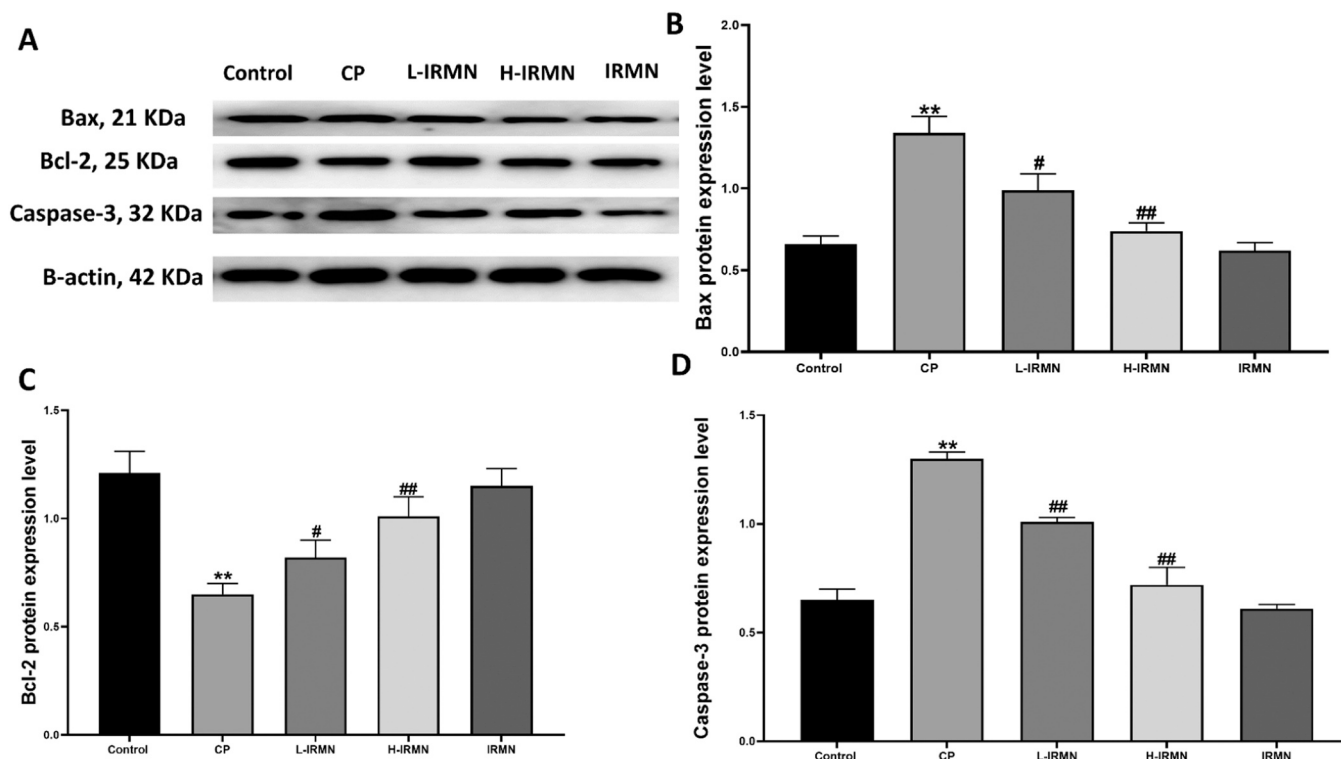


Fig. 8. : The influence of IRMN on the levels of apoptosis factors, including Bax (B), Bcl-2 (C), and Caspase-3 (D), in mice induced with CP (A). The data are presented as the mean ± SD for each group (n = 3). ** p < 0.01 compared to the CONT group; # p < 0.05 and ## p < 0.01 compared to the CP group.

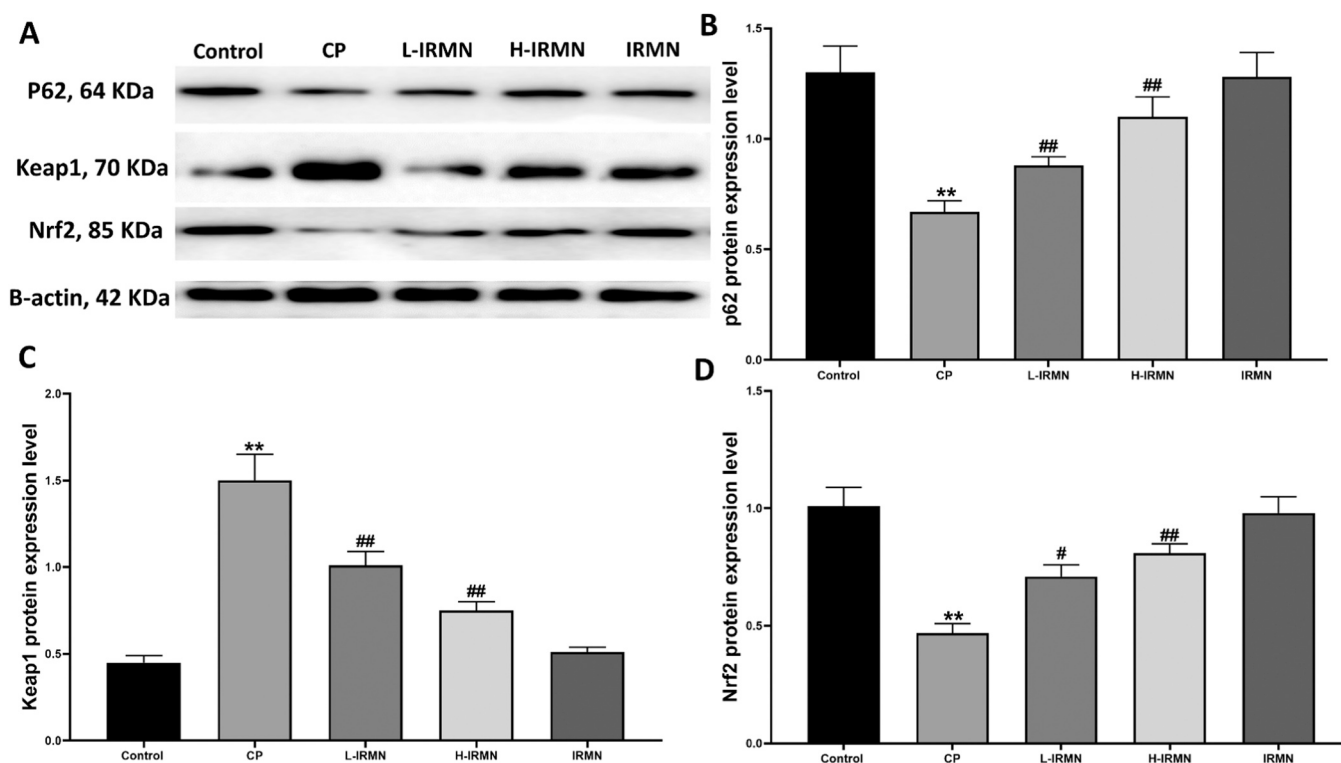


Fig. 9. : The impact of IRMN on the levels of signal pathway proteins, including p62 (B), Keap1 (C), and Nrf2 (D), in mice induced with CP (A). The data are presented as the mean ± SD for each group (n = 10). ** p < 0.01 compared to the CONT group; # p < 0.05 and ## p < 0.01 compared to the CP group.

triggering mitochondria-mediated cell death [39]. The accumulation of ROS due to CP can impair the function of heart mitochondria, leading to the release of factors that promote cell death. The Bcl-2 protein family,

which plays a critical role in controlling cell death, includes both anti-apoptotic (Bcl-2) and pro-apoptotic (Bax) proteins. While Bcl-2 helps maintain mitochondrial integrity, CP-induced ROS production

causes Bax to move to the mitochondria's outer membrane, activating Caspase-3, a key player in the cell death pathway, leading to apoptosis [40]. Our study's Western blot analysis showed a significant rise in Bax and Caspase-3 and a decrease in Bcl-2 in the CP group. Isorhamnetin treatment significantly reversed these changes, suggesting it could reduce heart toxicity by preventing cell death.

Oxidatively induced stress can activate transcription of various pro-inflammatory cytokines, with the ensuing inflammatory response potentially leading to cardiac damage. Moreover, this inflammation can exacerbate oxidative stress, which is also a significant trigger for programmed cell death. Most signals for apoptosis originate from the mitochondria, with the endogenous mitochondrial pathway being activated by various stimuli, including oxidative stress.

The regulation of oxidative stress features prominently the Keap1–Nrf2 pathway, a critical antioxidant defense mechanism [41]. Typically, Nrf2 is kept inactive in the cytoplasm through its association with Keap1 [42]. Under stress, this complex dissociates, liberating Nrf2 from Keap1's inhibitory influence, allowing it to activate and move to the nucleus. Nrf2 then becomes a central regulator of downstream antioxidant enzymes, activating superoxide dismutase (SOD) and catalase (CAT) to protect myocardial cells from oxidative damage [43].

Recent findings indicate that p62 plays a role in the regulation of oxidative stress via the Keap1–Nrf2 pathway [44]. The interaction between p62 and Keap1 enhances Nrf2's nuclear translocation and its downstream signaling pathway. In our research, CP treatment significantly decreased levels of p62 and Nrf2 while increasing Keap1 expression. Conversely, isorhamnetin treatment promoted the p62–Keap1 interaction, leading to an elevation in Nrf2 nuclear translocation, as evidenced by increased levels of p62 and Nrf2 and reduced Keap1 expression. This upregulation of Nrf2 led to heightened expression of antioxidant enzymes, thereby lowering ROS levels and alleviating CP-induced cardiac toxicity.

5. Limitations

This study acknowledges certain limitations in the methodologies employed. While we measured key apoptotic markers such as Bax, Bcl-2, and caspase-3 to assess apoptosis, the inclusion of the Annexin V/PI assay using flow cytometry would have provided a more direct and quantitative evaluation of the apoptotic rate. Similarly, although mitochondrial involvement in cardiac toxicity was highlighted, we were only able to measure ATP content, leaving mitochondrial membrane potential and cytochrome c levels unexplored. These aspects represent potential areas for future research, which could provide more comprehensive insights into the mechanistic underpinnings discussed. The study's conclusions are drawn within the context of these noted limitations, and we suggest these areas as fruitful directions for subsequent investigations.

6. Conclusion

In conclusion, Isorhamnetin (IRMN) demonstrates a substantial protective effect against cisplatin (CP)-induced cardiotoxicity. This protection is likely achieved through the inhibition of oxidative stress, inflammation, and apoptosis. The underlying mechanism appears to involve the activation of the p62–Keap1–Nrf2 signaling pathway. These results imply that Isorhamnetin holds promise as a protective agent against CP cardiotoxicity, potentially offering a valuable avenue for future anticancer clinical practice.

Funding

The authors would like to extend their sincere appreciation to the Deanship of Scientific Research at the Hashemite University, Zarqa, Jordan. (Grant number: 49/2020).

CRedit authorship contribution statement

Rawan AbuDalo: Writing – original draft, Conceptualization. **Omar Gammo:** Software. **Sara Altaber:** Resources. **Yusra Bseiso:** Investigation. **Esam Qnais:** Supervision, Project administration, Methodology, Formal analysis. **Mohammed Wedyan:** Visualization. **Muna Oqal:** Validation. **Abdelrahim Alqudah:** Writing – review & editing, Validation, Funding acquisition, Conceptualization.

Declaration of Competing Interest

The authors declare that they have no known competing financial interests or personal relationships that could have appeared to influence the work reported in this paper.

Data Availability

Data will be made available on request.

Acknowledgments

The authors would like to thank the Deanship of Scientific Research at the Hashemite University for sponsoring this research.

References

- [1] N. Devarajan, R. Manjunathan, S.K. Ganesan, Tumor hypoxia: the major culprit behind cisplatin resistance in cancer patients, *Crit. Rev. Oncol. Hematol.* 162 (2021) 103327, <https://doi.org/10.1016/J.CRITREVO.2021.103327>.
- [2] K.J.M. Schimmel, D.J. Richel, R.B.A. van den Brink, H.J. Guchelaar, Cardiotoxicity of cytotoxic drugs, *Cancer Treat. Rev.* 30 (2004) 181–191, <https://doi.org/10.1016/J.CTRV.2003.07.003>.
- [3] G.J. Dugbartey, L.J. Peppone, I.A.M. de Graaf, An integrative view of cisplatin-induced renal and cardiac toxicities: molecular mechanisms, current treatment challenges and potential protective measures, *Toxicology* 371 (2016) 58–66, <https://doi.org/10.1016/J.TOX.2016.10.001>.
- [4] X. Huang, D. He, Z. Pan, G. Luo, J. Deng, Reactive-oxygen-species-scavenging nanomaterials for resolving inflammation, *Mater. Today Biol.* 11 (2021) 100124, <https://doi.org/10.1016/J.MTBIO.2021.100124>.
- [5] A.F. Soliman, L.M. Anees, D.M. Ibrahim, Cardioprotective effect of zingerone against oxidative stress, inflammation, and apoptosis induced by cisplatin or gamma radiation in rats, *Naunyn. Schmiede Arch. Pharmacol.* 391 (2018) 819–832, <https://doi.org/10.1007/S00210-018-1506-4/FIGURES/5>.
- [6] P. Qian, L.J. Yan, Y.Q. Li, H.T. Yang, H.Y. Duan, J.T. Wu, X.W. Fan, S.L. Wang, Cyanidin ameliorates cisplatin-induced cardiotoxicity via inhibition of ROS-mediated apoptosis, *Exp. Ther. Med.* 15 (2018) 1959–1965, <https://doi.org/10.3892/ETM.2017.5617/HTML>.
- [7] C.T. Tan, H. Chang, Q. Zhou, C. Yu, N.Y. Fu, K. Sabapathy, V.C. Yu, MOAP-1-mediated dissociation of p62/SQSTM1 bodies releases Keap1 and suppresses Nrf2 signaling, *EMBO Rep.* 22 (2021). (https://doi.org/10.15252/EMBR.202050854/SUPPL_FILE/EMBR202050854-SUP-0011-SDATAEV.ZIP).
- [8] J.W. Kaspar, S.K. Niture, A.K. Jaiswal, Nrf2:INrf2 (Keap1) signaling in oxidative stress, *Free Radic. Biol. Med.* 47 (2009) 1304–1309, <https://doi.org/10.1016/J.FREERADBIOMED.2009.07.035>.
- [9] L. Gao, R. Yao, Y. Liu, Z. Wang, Z. Huang, B. Du, D. Zhang, L. Wu, L. Xiao, Y. Zhang, Isorhamnetin protects against cardiac hypertrophy through blocking PI3K–AKT pathway, *Mol. Cell. Biochem.* 429 (2017) 167–177, <https://doi.org/10.1007/S11010-017-2944-X/FIGURES/6>.
- [10] Y. Xu, C. Tang, S. Tan, J. Duan, H. Tian, Y. Yang, Cardioprotective effect of isorhamnetin against myocardial ischemia reperfusion (I/R) injury in isolated rat heart through attenuation of apoptosis, *J. Cell. Mol. Med.* 24 (2020) 6253–6262, <https://doi.org/10.1111/JCMM.15267>.
- [11] S. Ghafouri-Fard, A. Askari, H. Shoorai, M. Seify, Y. Koohestanidehagh, B. M. Hussen, M. Taheri, M. Samsami, Antioxidant therapy against TGF-β/SMAD pathway involved in organ fibrosis, *J. Cell. Mol. Med.* 28 (2024) e18052, <https://doi.org/10.1111/JCMM.18052>.
- [12] arrive, Home | ARRIVE Guidelines, (n.d.). (<https://arriveguidelines.org/>) (accessed October 3, 2023).
- [13] M. Perše, Cisplatin mouse models: treatment, toxicity and translatability, *Biomedicines* 9 (2021) 1406, <https://doi.org/10.3390/BIOMEDICINES9101406/S1>.
- [14] M. González-Arceo, I. Gomez-Lopez, H. Carr-Ugarte, I. Eseberri, M. González, M. P. Cano, M.P. Portillo, S. Gómez-Zorita, Anti-obesity effects of isorhamnetin and isorhamnetin conjugates, 24 (2022) 299, *Int. J. Mol. Sci.* Vol. 24 (2023) 299, <https://doi.org/10.3390/IJMS24010299>.
- [15] A.A. Grosset, K. Loayza-Vega, É. Adam-Granger, M. Birlea, B. Gilks, B. Nguyen, G. Soucy, D. Tran-Thanh, R. Albadine, D. Trudel, Hematoxylin and eosin counterstaining protocol for immunohistochemistry interpretation and diagnosis,

- Appl. Immunohistochem. Mol. Morphol. 27 (2019) 558–563, <https://doi.org/10.1097/PAI.0000000000000626>.
- [16] B. Rathkolb, W. Hans, C. Prehn, H. Fuchs, V. Gailus-Durner, B. Aigner, J. Adamski, E. Wolf, M.H. de Angelis, Clinical chemistry and other laboratory tests on mouse plasma or serum, *Curr. Protoc. Mouse Biol.* 3 (2013) 69–100, <https://doi.org/10.1002/9780470942390.MO130043>.
- [17] M.E. Mohamed, R.M. Abdelnaby, N.S. Younis, β -caryophyllene ameliorates hepatic ischemia reperfusion-induced injury: the involvement of Keap1/Nrf2/HO 1/NQO 1 and TLR4/NF- κ B/NLRP3 signaling pathways, *Eur. Rev. Med. Pharmacol. Sci.* 26 (2022) 8551–8566, <https://doi.org/10.26355/eurev.202211.30391>.
- [18] A. Boulinguez, C. Duhem, A. Mayeuf-Louchart, B. Pourcet, Y. Sebti, K. Kondratska, V. Montel, S. Delhay, Q. Thorel, J. Beauchamp, A. Hebras, M. Gimenez, M. Couvelaere, M. Zecchin, L. Ferri, N. Prevarskaya, A. Forand, C. Gentil, J. Ohana, F. Piétri-Rouxel, B. Bastide, B. Stael, H. Duez, S. Lancel, NR1D1 controls skeletal muscle calcium homeostasis through myoregulin repression, *JCI Insight* 7 (2022), <https://doi.org/10.1172/JCI.INSIGHT.153584>.
- [19] X. Liang, S. Ubhayakar, B.M. Liederer, B. Dean, A. Ran-Ran Qin, S. Shahidi-Latham, Y. Deng, Evaluation of homogenization techniques for the preparation of mouse tissue samples to support drug discovery, <https://doi.org/10.4155/Bio.11.181> 3 (2011) 1923–1933, <https://doi.org/10.4155/BIO.11.181>.
- [20] J.F. Kalinich, V.B. Vergara, J.F. Hoffman, Oxidative damage in metal fragment-embedded Sprague-Dawley rat gastrocnemius muscle, *Curr. Res. Toxicol.* 3 (2022), <https://doi.org/10.1016/J.CRTOX.2022.100083>.
- [21] J. Yang, J. Xu, L. Tao, S. Wang, H. Xiang, Y. Tang, Synergetic protective effect of remote ischemic preconditioning and prolyl 4-hydroxylase inhibition in ischemic cardiac injury, *Mol. Med. Rep.* 25 (2022), <https://doi.org/10.3892/MMR.2022.12596>.
- [22] Y.W. Wang, H.Z. Dong, Y.X. Tan, X. Bao, Y.M. Su, X. Li, F. Jiang, J. Liang, Z. C. Huang, Y.L. Ren, Y.L. Xu, Q. Su, HIF-1 α -regulated lncRNA-TUG1 promotes mitochondrial dysfunction and pyroptosis by directly binding to FUS in myocardial infarction, *Cell Death Discov.* 8 (2022), <https://doi.org/10.1038/S41420-022-00969-8>.
- [23] A. Alqudah, E.Y. Qnais, M.A. Wedyan, S. Altaber, R. Abudalo, O. Gammoh, H. Alkhateeb, S. Bataineh, R.Y. Athamneh, M. Oqal, K. Abu-Safieh, L. McClements, New treatment for type 2 diabetes mellitus using a novel bipyrazole compound, *12 (2023) 267*, *Cells* Vol. 12 (2023) 267, <https://doi.org/10.3390/CELLS12020267>.
- [24] H.M. Peshavariya, G.J. Dusting, S. Selemidis, Analysis of dihydroethidium fluorescence for the detection of intracellular and extracellular superoxide produced by NADPH oxidase, *Free Radic. Res.* (2007), <https://doi.org/10.1080/10715760701297354>.
- [25] G.N. Konstantinou, Enzyme-Linked Immunosorbent Assay (ELISA), *Methods Mol. Biol.* 1592 (2017) 79–94, https://doi.org/10.1007/978-1-4939-6925-8_7.
- [26] A. Alqudah, E. Qnais, M. Alqudah, O. Gammoh, M. Wedyan, S.S. Abdalla, Isorhamnetin as a potential therapeutic agent for diabetes mellitus through PGK1/AKT activation, *Arch. Physiol. Biochem.* (2024), <https://doi.org/10.1080/13813455.2024.2323947>.
- [27] E.S.E. El-Awady, Y.M. Moustafa, D.M. Abo-Elmatty, A. Radwan, Cisplatin-induced cardiotoxicity: Mechanisms and cardioprotective strategies, *Eur. J. Pharmacol.* 650 (2011) 335–341, <https://doi.org/10.1016/J.EJPHAR.2010.09.085>.
- [28] E.E. Gunturk, B. Yucel, I. Gunturk, C. Yazici, A. Yay, K. Kose, The effects of N-acetylcysteine on cisplatin induced cardiotoxicity, *Bratisl. Med. J.-BRATISLAVSKE Lek. List.* 120 (2019) 423–428, <https://doi.org/10.4149/BLL.2019.068>.
- [29] J.H. Yang, S.C. Kim, K.M. Kim, C.H. Jang, S.S. Cho, S.J. Kim, S.K. Ku, L.J. Cho, S. H. Ki, Isorhamnetin attenuates liver fibrosis by inhibiting TGF- β /Smad signaling and relieving oxidative stress, *Eur. J. Pharmacol.* 783 (2016) 92–102, <https://doi.org/10.1016/J.EJPHAR.2016.04.042>.
- [30] B. Yang, X.P. Li, Y.F. Ni, H.Y. Du, R. Wang, M.J. Li, W.C. Wang, M.M. Li, X. H. Wang, L. Li, W.D. Zhang, T. Jiang, Protective effect of isorhamnetin on lipopolysaccharide-induced acute lung injury in mice, *Inflammation* 39 (2016) 129–137, <https://doi.org/10.1007/S10753-015-0231-0/FIGURES/7>.
- [31] J. Jian, L. Yu-Qing, H. Rang-Yue, Z. Xia, X. Ke-Huan, Y. Ying, W. Li, T. Rui-zhi, Isorhamnetin ameliorates cisplatin-induced acute kidney injury in mice by activating SLP1-mediated anti-inflammatory effect in macrophage, *Immunopharmacol. Immunotoxicol.* (2024) 1–11, <https://doi.org/10.1080/08923973.2024.2329621>.
- [32] Y.A. Khadrawy, E.N. Hosny, M.M. El-Gizawy, H.G. Sawie, H.S. Aboul, The effect of curcumin nanoparticles on cisplatin-induced cardiotoxicity in male wistar albino rats, *Cardiovasc. Toxicol.* 21 (2021) 433–443, <https://doi.org/10.1007/S12012-021-09636-3/FIGURES/4>.
- [33] L.M. Gregg Antunes, J.D. arc C. Darin, M.D.L.P. Bianchi, Protective effects of vitamin C against cisplatin-induced nephrotoxicity and lipid peroxidation in adult rats: a dose-dependent study, *Pharmacol. Res.* 41 (2000) 405–411, <https://doi.org/10.1006/PHRS.1999.0600>.
- [34] V.P. Vineetha, K.G. Raghu, An overview on arsenic trioxide-induced cardiotoxicity (2019), *Cardiovasc. Toxicol.* 192 (19) (2019) 105–119, <https://doi.org/10.1007/S12012-018-09504-7>.
- [35] J. Liu, G. Chang, J. Huang, Y. Wang, N. Ma, A.C. Roy, X. Shen, Sodium butyrate inhibits the inflammation of lipopolysaccharide-induced acute lung injury in mice by regulating the toll-like receptor 4/nuclear factor κ B signaling pathway, *J. Agric. Food Chem.* (2019). (<https://doi.org/10.1021/ACS.JAFC.8B06359/ASSET/IMAGES/MEDIUM/JF-2018-06359Z.0005.GIF>).
- [36] Resveratrol attenuates inflammation in the rat heart subjected to ischemia-reperfusion: Role of the TLR4/NF- κ B signaling pathway, (n.d.). (<https://www.spandidos-publications.com/10.3892/mmr.2014.2955?text=abstract>) (accessed March 26, 2024).
- [37] I. Mikaelian, D. Coluccio, K.T. Morgan, T. Johnson, A.L. Ryan, E. Rasmussen, R. Nicklaus, C. Kanwal, H. Hilton, K. Frank, L. Fritzky, E.B. Wheelton, Temporal gene expression profiling indicates early up-regulation of interleukin-6 in isoproterenol-induced myocardial necrosis in rat, <http://Dx.Doi.Org/10.1177/0192623307312696> 36 (2008) 256–264, <https://doi.org/10.1177/0192623307312696>.
- [38] A.A. Al-Majed, M.M. Sayed-Ahmed, A.A. Al-Yahya, A.M. Aleisa, S.S. Al-Rejaie, O. A. Al-Shabanah, Propionyl-L-carnitine prevents the progression of cisplatin-induced cardiomyopathy in a carnitine-depleted rat model, *Pharmacol. Res.* 53 (2006) 278–286, <https://doi.org/10.1016/J.PHRS.2005.12.005>.
- [39] Z.V. Varga, P. Ferdinandy, L. Liaudet, P. Pacher, Drug-induced mitochondrial dysfunction and cardiotoxicity, *Am. J. Physiol. - Hear. Circ. Physiol.* 309 (2015) H1453–H1467. (<https://doi.org/10.1152/AJPHEART.00554.2015/ASSET/IMAGES/LARGE/ZH40211517120005.JPEG>).
- [40] E.A. Kosenko, I.N. Solomadin, L.A. Tikhonova, V. Prakash Reddy, G. Aliev, Y.G. Kaminsky, Pathogenesis of Alzheimer Disease: Role of Oxidative Stress, Amyloid- β Peptides, Systemic Ammonia and Erythrocyte Energy Metabolism, (n.d.).
- [41] P. Canning, F.J. Sorrell, A.N. Bullock, Structural basis of Keap1 interactions with Nrf2, *Free Radic. Biol. Med.* 88 (2015) 101–107, <https://doi.org/10.1016/J.FREERADBIOMED.2015.05.034>.
- [42] C.A. Silva-Islas, P.D. Maldonado, Canonical and non-canonical mechanisms of Nrf2 activation, *Pharmacol. Res.* 134 (2018) 92–99, <https://doi.org/10.1016/J.PHRS.2018.06.013>.
- [43] L. Zhao, Protective effects of trimetazidine and coenzyme Q10 on cisplatin-induced cardiotoxicity by alleviating oxidative stress and mitochondrial dysfunction, *Anatol. J. Cardiol.* 22 (2019) 232–239, <https://doi.org/10.14744/AnatolJCardiol.2019.83710>.
- [44] D. Bartolini, K. Dallaglio, P. Torquato, M. Piroddi, F. Galli, Nrf2-p62 autophagy pathway and its response to oxidative stress in hepatocellular carcinoma, *Transl. Res.* 193 (2018) 54–71, <https://doi.org/10.1016/J.TRSL.2017.11.007>.
- [45] G. Gong, Y.Y. Guan, Z.L. Zhang, K. Rahman, S.J. Wang, S. Zhou, X. Luan, H. Zhang, Isorhamnetin: a review of pharmacological effects, *Biomed. Pharmacother.* 128 (2020) 110301, <https://doi.org/10.1016/J.BIOPHA.2020.110301>.